# Isomerization Couples Chemistry in the ATP Sulfurylase-GTPase System†

Jiang Wei and Thomas S. Leyh*

*Department of Biochemistry, Albert Einstein College of Medicine, 1300 Morris Park Avenue, Bronx, New York 10461*

*Received January 28, 1999; Revised Manuscript Received March 19, 1999*

ABSTRACT: ATP sulfurylase catalyzes and couples the free energies of two reactions: GTP hydrolysis and the synthesis of activated sulfate, or APS. The GTPase active site undergoes changes during its catalytic cycle that are driven by events that occur at the APS-forming active site, which is located in a separate subunit. GTP responds to its changing environment by moving along its reaction path. The response, which may change the affinity or reactivity of GTP, can, in turn, produce alterations at the APS active site that drive APS synthesis. The resulting stepwise progression of the two reactions couples their free energies. The mechanism of ATP sulfurylase involves an enzyme isomerization that precedes and rate limits cleavage of the $\beta,\gamma$-bond of GTP. These fluorescence studies demonstrate that the isomerization is controlled by the binding of activators that drive ATP sulfurylase into forms that mimic different stages of the APS reaction. Only certain activators elicit the isomerization, suggesting that the APS reaction must proceed to a specific point in the catalytic cycle before the conformational "switch" that controls GTP hydrolysis is thrown. The isomerization is shown to require occupancy of the $\gamma$-phosphate subsite of the GTP binding pocket. This requirement establishes that the isomerization results in a change in the interaction between the enzyme and the $\gamma$-phosphate of GTP that emerges in the catalytic cycle during the transition from the nonisomerized to the isomerized E·GTP complex. The newly formed contact(s) appears to carry into the bond-breaking transition state, and to be essential for the enhanced affinity and reactivity of the nucleotide.

Coupling changes in the structural and functional properties of one region of an enzyme to the steps of an energy-producing reaction that occurs at a separate site on the enzyme is a versatile form of energy linkage (*1*). Such mechanisms drive the macromolecular motion that results in the supercoiling of DNA (*2*, *3*), the movement of cellular cargo along cytoskeletal roadways (*4*), the transport of an ion across a membrane (*5*, *6*), and the ratcheting of the S1 head of myosin along F-actin fibers that results in muscle contraction (*7*, *8*). In seemingly rare situations, conformational coupling links the energetics of separate small molecule reactions to one another. Such is the case with the enzyme ATP sulfurylase (ATP:sulfate adenylyltransferase, EC 2.7.7.4) from *Escherichia coli* K-12.

ATP sulfurylase is a GTPase−target complex that conformationally couples the Gibbs potentials of GTP hydrolysis and activated sulfate [adenosine 5′-phosphosulfate (APS)[1]] synthesis (reactions 1 and 2) (*9*, *10*).

$$ATP + SO_4 \rightleftharpoons APS + PP_i \quad (1)$$

$$GTP + H_2O \rightleftharpoons GDP + P_i + H^+ \quad (2)$$

The enzyme is a tetramer of heterodimers. One of the dimer's subunits, CysN (53 kDa), is the GTPase; the other, CysD (23 kDa), contains the active site for APS synthesis (*11*). GTP hydrolysis thermodynamically drives the extremely unfavorable transfer of the adenylyl moiety from pyrophosphate to sulfate [$\Delta G^{\circ\prime} \sim 10$ kcal/mol (*12*, *13*)]. The resultant phosphoric−sulfuric acid anhydride bond, the chemical hallmark of activated sulfate, potentiates the sulfuryl group for transfer to cellular recipients. This transfer reaction regulates a variety of cellular processes, including (*13*) estrogen receptor activation (*14*, *15*), lymph cell circulation (*16*), and hemophilia B (*17*).

The current model for energetic coupling in ATP sulfurylase suggests that the arrival of the APS-forming reaction at, or near, the E*AMP·$PP_i$ intermediate that occurs in the catalytic cycle initiates an isomerization of the enzyme that accelerates GTP hydrolysis (*18*). This model is considerably expanded in this paper. It is possible to form ligand complexes with ATP sulfurylase that mimic various stages of the APS-forming reaction. Similarly, substrate, transition-state, and product complexes of the GTPase reaction can be formed. To identify the combinations of complexes which elicit the isomerization, these sets of complexes were experimentally crossed using the fluorescence of mant-nucleotide analogues to monitor the isomerization and guanine nucleotide affinity changes associated with each complex. The results demonstrate that the isomerization, which occurs after the binding of guanine nucleotide, hinges upon changes in the interaction of the enzyme and the $\gamma$-phosphate of GTP. The altered $\gamma$-phosphate contact(s) appears to carry from the ground-state isomerized complex into the transition state.

† Supported by National Institutes of Health Grant GM 54469.

* To whom correspondence should be addressed: Department of Biochemistry, Albert Einstein College of Medicine, 1300 Morris Park Ave., Bronx, NY 10461. Telephone: (718) 430-2857. Fax: (718) 430-8565. E-mail: Leyh@aecom.yu.edu.

[1] Abbreviations: Tris, tris(hydroxymethyl)aminomethane; unit, micromoles of substrate converted to product per minute at $V_{max}$; m or mant, *O*-(*N*-methylanthraniloy)-2′-deoxy.

10.1021/bi990216h CCC: $18.00 
Published on Web 04/21/1999

Table 1: Dissociation Constants[a] for the Binding of Guanine Nucleotide to Ground- and Transition-State Complexes of ATP Sulfurylase

| Complex | $K_{d(app)}$ ($\mu$M)[b] | $(I_c/I_s)$[c] |
|---|---|---|
| **E**·mGDP | 9.7 | 1.5 |
| AMP·$PP_i$·**E**·mGDP | 14 | 1.4 |
| AMP·$PP_i$·$AlF_x$·**E**·mGDP | 0.061 | 1.4 |
| **E**·mGMPPNP | 27 | 2.0 |
| $PP_i$·**E**·mGMPPNP | 37 | 1.7 |
| AMP·**E**·mGMPPNP | 0.47 | 1.5 |
| AMP·$PP_i$·**E**·mGMPPNP | 0.0058 | 2.6 |

[a] The dissociation constants were obtained by fitting fluorescence titration data to a single-step binding model. [b] The $K_d$ standard errors, given in percent of $K_d$, are, from top to bottom, 12, 9, 20, 7, 11, 15, and 16%. [c] $I_c/I_s$ represents the ratio of the fluorescent intensity of the nucleotide in the enzyme complex to that in solution. The errors associated with $I_c/I_s$ were <0.1 in all cases.

## MATERIALS AND METHODS

*Materials.* The synthesis and purification of fluorescent guanine nucleotide analogues mGMPPNP [3′-*O*-(*N*-methylanthraniloyl)-2′-deoxyguanosine 5′-[$\beta,\gamma$-imido]triphosphate] and mGDP [3′-*O*-(*N*-methylanthraniloyl)-2′-deoxyguanosine 5′-diphosphate] have been described previously (*19*, *20*). AMP (free acid), $MgCl_2$, $Na_4PP_i$, NaF, and Tris[1] were purchased from Sigma Chemical Co.

*ATP Sulfurylase.* The native *E. coli* ATP sulfurylase used in these studies is purified from an *E. coli* strain, containing an expression plasmid, that produces the enzyme at high levels (*20*). The specific activity of the ATP sulfurylase, assayed according to a published protocol, was 0.74 unit/mg (*21*).

*Fluorescence Titrations.* Titrations were performed by monitoring the change in fluorescent intensity that occurred upon dilution of solutions containing the highest concentration of titrant (i.e., enzyme) with a concentration-matched solution that did not contain titrant. The fluorescence measurements were taken using a Proton Technology International QM-1 spectrometer with a xenon compact arc lamp and a 710 Photomultiplier Detection System. The mant compounds were excited at 350 nm (2 nm entrance slit); the emitted light was detected at 450 nm (10 nm exit slit).

The protocol and conditions for the binding studies associated with Table 1 are discussed here. Tris buffer (50 mM, pH/HCl = 8.0) was used in all of the titrations. The solutions were equilibrated, and the titrations were performed at 25 ± 2 °C. The $MgCl_2$ concentration was maintained at [nucleotide] + [$PP_i$] + 1.0 mM. Two to five intensity measurements, taken at each titrant concentration, were averaged to obtain the intensity at that concentration. Each titration was performed at least twice. The data were averaged and fit using a single-site binding model. The titrant concentrations typically ranged from $0.1K_d$ to $5K_d$. A representative titration is shown in Figure 1. The conditions of each of the titrations are discussed in the following list in the order in which they appear in Table 1 (top to bottom): (1) the binding of mGDP to E ([mGDP] = 1.0 $\mu$M), (2) the binding of mGDP to E·AMP·$PP_i$ ([mGDP] = 1.0 $\mu$M, [AMP] = 1.0 or 5.0 mM, and [$PP_i$] = 1.0 mM.) This experiment was performed at 1.0 and 5.0 mM AMP to assess whether the AMP concentration was saturating; the mGDP $K_d$s at these concentrations were identical, within experimental error, (3) the E·AMP·$PP_i$·$AlF_x$ complex ([mGDP] = 0.1 $\mu$M, [AMP] = 1.0 mM, [$PP_i$] = 0.50 mM, [$AlF_x$] = 30 $\mu$M, and [NaF] = 10 mM.) Experimentally accessible concentrations of $AlF_x$ have no effect on the binding or emitted intensity of E·mGDP; hence, it is not feasible to saturate the E·mGDP complex with $AlF_x$. This prevents determining the affinity of AMP and/or $PP_i$ for the E·mGDP·$AlF_x$ complex. To confirm that the AMP (1.0 mM) and $PP_i$ (0.50 mM) concentrations used in the data depicted in panel B of Figure 3 were at, or near, saturation, the $K_d$ of mGDP was shown to be the same at higher concentrations of these ligands, (4) the binding of mGMPPNP to E (see the legend of Figure 1), (5) the binding of mGMPPNP to E·$PP_i$ ([mGMPPNP] = 0.50 $\mu$M and [$PP_i$] = 1.0 mM, $22K_d$ (*24*)), (6) the binding of mGMPPNP to E·AMP ([mGMPPNP] = 0.50 $\mu$M and [AMP] = 5.0 mM, $8.3K_d$ (*22*)), and (7) the binding of mGMPPNP to E·AMP·$PP_i$ ([mGMPPNP] = 0.10 $\mu$M, [$PP_i$] = 200 $\mu$M, $2900K_d$; [AMP] = 1.0 mM, $7800K_d$). The $K_d$ values for $PP_i$ (69 nM) and AMP (127 nM) for the E·AMP·$PP_i$ complex were determined (data not shown) to ensure that these activators were at saturation in titrations 5−7.

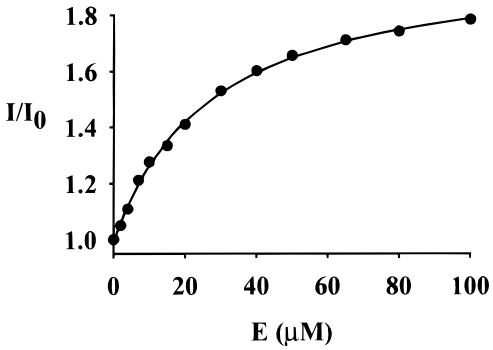


FIGURE 1: Binding of mGMPPNP to ATP sulfurylase. The solution composition was as follows: ATP sulfurylase (at the indicated concentration), mGMPPNP (0.50 $\mu$M), Tris (50 mM, pH 8.0), and $MgCl_2$ ([nucleotide] + 1.0 mM). Titrations were performed by dilution of a solution containing enzyme with a concentration-matched solution that did not contain enzyme. The solutions were maintained at 25 ± 2 °C during the titrations. Each dot represents the average of at least two independent measurements. The solid line represents the binding curve predicted by the best-fit binding parameters obtained using a single-site binding model; the parameters are compiled in Table 1.

*Fitting the Titration Data.* The titrations were curve-fit using the Sigma Plot program which uses the Marquardt−Levenberg fitting algorithm. The single-site binding model used to fit the data is described by a second-order polynomial, the root of which was used to fit the data and obtain the binding constants.

## RESULTS AND DISCUSSION

*Ground-State Complexes.* Unlike the p21-style GTPases whose hydrolytic activities are regulated by proteins, GAPs and GNRPs (*23*, *24*), the activity of ATP sulfurylase is regulated by small molecules: the reactants and reactant analogues of the APS-forming reaction (*19*, *25*). Together, the activators AMP and $PP_i$ elicit a form of ATP sulfurylase that functionally resembles the E*AMP·$PP_i$ intermediate that forms during the catalytic cycle (*10*). Stopped-flow fluores-

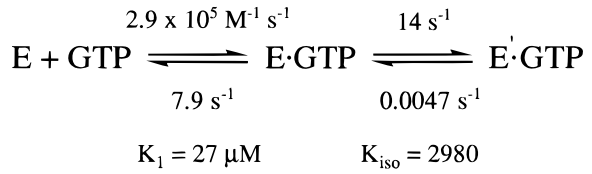


FIGURE 2: Two-step mechanism for the binding of GTP to ATP sulfurylase. E represents the AMP·$PP_i$ complex of ATP sulfurylase, and the prime denotes the isomerized form of this complex. The isomerization step rate limits cleavage of the $\beta,\gamma$-bond of GTP. The equilibrium constants, $K_1$ and $K_{iso}$, were calculated from the rate constants for the individual steps, which were determined in a previous study (*18*).

cence studies have revealed that the fluorescent analogues of GTP, mGMPPNP [3′-*O*-(*N*-methylanthraniloyl)-2′-deoxyguanosine 5′-[$\beta,\gamma$-imido]triphosphate] and mGTP, bind to the E·AMP·$PP_i$ complex in at least two steps (*18*). The end product of the first step, the mGTP·E·AMP·$PP_i$ complex, undergoes an isomerization, to the mGTP·E′·AMP·$PP_i$ complex, that rate limits cleavage of the $\beta,\gamma$-bond of GTP. This ligand-induced isomerization is quite favorable [$K_{iso} = 3000$ ($\Delta G° = -4.7$ kcal/mol)] and is a key event in linking the Gibbs potentials of these two reactions (*18*).

To better understand how the binding and isomerization properties of the E·$PP_i$·AMP complex develop from its precursor complexes, the affinities of mGMPPNP for E, E·$PP_i$, E·AMP, and E·AMP·$PP_i$ were determined by fluorescence titration at 25 ± 2 °C (see Materials and Methods). The titrations were fit using a single-step binding model, and the resulting apparent dissociation constants are compiled in Table 1. A representative titration is shown in panel A of Figure 1. The one-step binding model can accurately predict the behavior of binding reactions involving multiple steps. In the case of two-step binding, the apparent constant, $K_{d(app)}$, obtained from a one-step fit is related to the equilibrium constants for the forward, first, and second steps of the two-step process, $K_1$ and $K_{iso}$ (see Figure 2), respectively, by eq 3.

$$K_{d(app)} = ([E]\cdot[L])/([E\cdot L] + [E'\cdot L]) = 1/(K_1 + K_1K_{iso}) \quad (3)$$

$K_1$ and $K_{iso}$ for the binding of mGMPPNP to the E·$PP_i$·AMP complex are $3.7 \times 10^4$ M and 3000, respectively (*18*). The $K_{d(app)}$ calculated using these values and eq 3 ($9.0 \times 10^{-9}$ M) agrees reasonably well with the experimentally determined value ($5.8 \times 10^{-9}$ M) (Table 1).

$K_{d(app)}$ values for the binding of mGMPPNP to E and E·$PP_i$ are similar to one another (27 ± 1.9 and 37 ± 4.1 $\mu$M, respectively) and to $K_1$ for the binding of mGMPPNP to the nonisomerized E·$PP_i$·AMP complex [27 ± 5 $\mu$M (*18*)]. These similarities suggest that neither the mGMPPNP·E nor the mGMPPNP·E·$PP_i$ complex isomerizes significantly and that the affinity of the nonisomerized enzyme for the nucleotide is virtually independent of the activator. Thus, the activator specific interactions between the sites appear to be associated with the isomerization itself.

$K_{d(app)}$ for the AMP·E·mGMPPNP complex (470 nM) is remarkably small compared to this "same" dissociation constant measured by either initial rate or pre-steady-state methods. The $K_m$ of GTP for the E·AMP complex (24 ± 0.4 $\mu$M) should be an excellent approximation of $K_d$ since isotope tapping and partition experiments have shown that the binding of GTP is near equilibrium during turnover (*24*). $k_{on}$ and $k_{off}$ for the mGTP−E·AMP interactions, obtained from pre-steady-state fluorescence measurements (*19*), predict a $K_d$ for the mGTP·E·AMP complex of 21 ± 1.1 $\mu$M. The similar behavior of mGTP and mGMPPNP toward the E·AMP·$PP_i$ complex suggests that the low $K_d$ of mGMPPNP for the E·AMP complex is not due to its $\beta,\gamma$-imido linkage.

The explanation for the discrepancy in nucleotide affinity lies in the different conditions under which the measurements were taken. The $K_{d(app)}$ values were obtained from measurements of the system at equilibrium, and are given by eq 3. $K_m$ and $K_d$ were obtained from nonequilibrium measurements. $K_m$ was determined under initial rate conditions at a saturating AMP concentration. Under these conditions, the GTP hydrolysis mechanism can be represented by eq 4 in which the enzyme (i.e., E·AMP) binds substrate, isomerizes, and forms products which are released in an irreversible step. The substrate $K_m$ associated with the mechanism outlined in eq 4 is given by eq 5 (*26*) which reveals that as $k_3$ (the rate constant for the forward isomerization step) approaches zero, the binding of substrate to the nonisomerized form of the enzyme approaches equilibrium and, therefore, $K_m$ approaches $K_d$ for that step.

$$E + S \underset{k_2}{\overset{k_1}{\rightleftharpoons}} E\cdot S \underset{k_4}{\overset{k_3}{\rightleftharpoons}} E'\cdot S \underset{k_6}{\overset{k_5}{\rightleftharpoons}} E'\cdot P \xrightarrow{k_7} E + P \quad (4)$$

$$K_m = \frac{k_2\,(k_4k_6 + k_4k_7 + k_5k_7) + k_3\,(k_5k_7)}{k_1\,(k_4k_6 + k_4k_7 + k_5k_7) + k_3\,(k_1k_5 + k_2(k_6 + k_7))} \quad (5)$$

$K_d$ for mGTP binding to E·AMP was determined from the enzyme concentration dependence of the fast phase of a biphasic reaction in which the first or fast phase monitors binding of the nucleotide, in this case, to the nonisomerized form of the enzyme. The second phase monitors $\beta,\gamma$-bond breaking. Thus, in the case of a mechanism in which a slow isomerization immediately follows substrate binding, these equilibrium and nonequilibrium measurements probe different regions of the binding reaction. The nonequilibrium measurements probe binding to the nonisomerized enzyme form, whereas the equilibrium measurements are influenced by both the binding and isomerization steps.

The nucleotide affinities for the E·AMP complex measured by steady-state and pre-steady-state methods (24 and 21 $\mu$M, respectively) are in close agreement with that for the nonisomerized E·AMP·$PP_i$ complex (27 $\mu$M), again suggesting the activator independence of the interactions of the nonisomerized form of the enzyme with nucleotide. The $K_{d(app)}$ values for these two complexes, however, are very different (470 and 5.8 nM, respectively). Hence, the activator specific binding interactions between the nucleotide and its active site must appear in the mechanism after forming the nonisomerized complex. If the isomerization were to occur in a single step, as is allowed by the two-step model, the structural features of the enzyme that interact with the activator(s) must emerge during that step. The stabilization of these emerging features by interaction with the activators will accelerate the rate of isomerization (and therefore $\beta,\gamma$-bond cleavage), and stabilization of these, and perhaps additional features in the ground state, will shift the isomer-

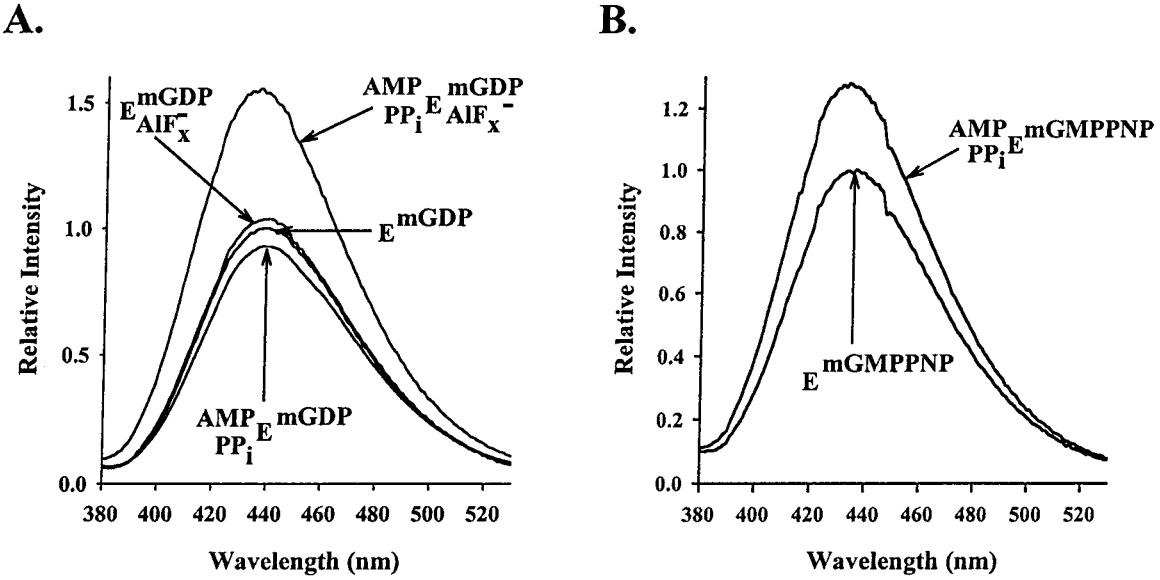


FIGURE 3: Effects of AMP−$PP_i$ binding and $AlF_x$ transition-state complex formation on the emission spectra of enzyme-bound mGDP and mGMPPNP. (A) The enzyme-bound mGDP emission spectra. The conditions were as follows: mGDP (2.0 $\mu$M), ATP sulfurylase (150 $\mu$M active sites), AMP (0 or 2.0 mM), $PP_i$ (0 or 200 $\mu$M), $MgCl_2$ ([nucleotide] + [$PP_i$] + 1.0 mM), Tris/HCl (50 mM, pH 8.0), $AlCl_3$ (0 or 30 $\mu$M), NaF (0 or 10 mM), and 25 ± 2 °C. (B) The mGMPPNP spectra. The conditions were as follows: mGMPPNP (2.0 $\mu$M) and ATP sulfurylase (250 $\mu$M active sites). The temperature and concentrations of all other species were identical to those associated with panel A. The concentration of activator(s) used in this study is $>8.2K_m$ in all cases.

ization equilibrium toward the isomerized complex.

The isomerization equilibrium constant (3000 for the E·AMP·$PP_i$ complex) can be calculated for the E·AMP complex. Using eq 3 and a $K_1$ value of 1/(23 $\mu$M), $K_{iso}$ for the E·AMP complex is calculated as 48. The ~60-fold difference between the $K_{iso}$ values for the E·AMP·$PP_i$ and E·AMP complexes is caused by the binding of $PP_i$ which alone does not significantly alter $K_{iso}$. Thus, certain mGMPPNP binding determinants are uniquely associated with the synergistic interactions of these activators. When this result is extrapolated to the native reaction, the release of $PP_i$, which occurs after formation of the E*AMP·$PP_i$ intermediate, appears to be associated with a partial reversal of the isomerization, or a "resetting" of the enzyme to its nonisomerized state.

*The Transition-State Complex.* $AlF_x$·nucleotide complexes have been used as transition-state analogues of phosphoryl transfer reactions in kinases and GTPases (*27*−*32*). Both the associative and dissociative phosphoryl transfer mechanisms involve an unstable planar, anionic phosphoryl species. This "in-flight" species is mimicked by the equatorial plane of the $Al^{3+}$ complex which is centered on $Al^{3+}$ and has a fluorine atom at each of its four corners. The incoming and departing groups of the reacting complex are imitated by the axial ligands of the $Al^{3+}$ complex, water, and the $\beta$-phosphoryl oxygen. While the functional consequences of $AlF_x$ in GTPase systems are often quite informative, the mass-action effects of the pertinent $Al^{3+}$ complexes cannot yet be accurately quantitated due to the complexity of the $Al^{3+}$ coordination chemistry. Aqueous solutions of $Al^{3+}$, fluoride, and nucleotide diphosphate, NDP, at neutral pH contain greater than 30 $Al^{3+}$ species (*33*); the NDP·$AlF_4$-$(H_2O)^{4-}$ complex is a minor species that, despite efforts (*34*), has not been quantitated.

To test for the formation of the $AlF_x$ transition-state complex at the GTPase active site of ATP sulfurylase, the influence of $AlF_x$ on the emission spectrum of enzyme-bound mGDP and on the affinity of mGDP for the E and E·AMP·$PP_i$ complexes was determined. The effects of $AlF_x$ on the emission spectrum of the E·mGDP and AMP·$PP_i$·E·mGDP complexes are shown in Figure 3A. For comparison, the effects of AMP·$PP_i$ on the emission spectrum of mGMPPNP are shown in Figure 3B. The concentration of ATP sulfurylase used in these experiments was such that >95% of the mGDP is bound to the enzyme. $AlF_x$ causes a substantial change in the spectrum of the AMP·$PP_i$·E·mGDP complex, while its effects on the E·mGDP complex are small. The combination of activator and $AlF_x$ binding causes the emission maximum of the E·mGDP complex to blue-shift 5 ± 1 nM, from 440 to 435 nm, and the emitted intensity to increase 53 and 56% at 440 and 435 nm, respectively. A smaller increase in emission intensity, 28%, and no detectable change in excitation maximum are observed for enzyme-bound mGMPPNP when the enzyme isomerizes (Figure 3B). The effects of $AlF_x$ on the affinity of mGDP parallel its effects on the emission spectrum. Neither the activators nor $AlF_x$ alone has a significant influence on the affinity of mGDP (Table 1); however, in combination, these ligands cause a 300-fold decrease in the apparent $K_d$ of mGDP, from 14 ± 3 $\mu$M to 61 ± 12 nM. Thus, the isomerization appears to be essential for forming the tightly bound transition-state complex, and as is the case for ground-state mGMPPNP complexes, it causes a significant increase in the emission intensity of the bound mGDP.

The affinity of mGDP is not significantly effected by AMP and $PP_i$ [$K_{d(app)}$ values with and without activators are 14 ± 3 and 9.7 ± 1 $\mu$M, respectively; see Table 1]. Hence, the enzyme cannot isomerize when mGDP alone occupies the binding site. However, when the $\gamma$-phosphoryl binding pocket of the mGDP·E·AMP·$PP_i$ complex is filled by $AlF_x$, the fluorescence changes (Figure 3A) and tight binding associated with the isomerization occur (Table 1). These data

suggest that the isomerization requires occupancy of the $\gamma$-phosphate binding pocket of the GTP active site. If it is empty, the interaction energy between the APS-forming and GTP-hydrolysis active sites moves to zero. Further evidence supporting the necessity of the $\gamma$-phosphoryl group for the isomerization is provided by the fact that mGMPPNP, which contains the $\gamma$-phosphoryl moiety, elicits the isomerization.

The simplest model consistent with the findings presented is one in which the guanine nucleotide and activators assemble a nonisomerized enzyme complex. The affinity of this complex for the guanine nucleotide is essentially the same, regardless of whether activators are bound. If the appropriate activators are bound, and the $\gamma$-phosphoryl subsite of the GTP binding pocket is occupied, the interactions between the active sites that drive the isomerization begin to occur. The site−site interaction continues through the ground state and into the $\beta,\gamma$-bond breaking transition state. The interactions cease at a point prior to forming the E·GDP complex, possibly at the phosphate release step. The allosteric circuitry, which controls GTP hydrolysis, is transiently engaged during this segment of the mechanism. The requirement that the $\gamma$-phosphoryl subsite be occupied to observe the interaction pinpoints the structural basis for the dependency to changes in the $\gamma$-phosphoryl subsite. This structural change dramatically enhances both the affinity and reactivity of the GTP. It is as if the isomerization has activated a catalytic residue(s) by bringing it into contact with the $\gamma$-phosphoryl group of GTP.

The spectral and functional changes associated with the binding of AMP and $PP_i$ to the E·mGDP complex resemble the changes that occur when the GTPase activating proteins (GAPs), neurofibromin or $p120^{GAP}$, bind to RAS·mGDP. GAP binding causes a 50% increase in the emitted intensity at $\lambda_{max}$, and an 18 nm blue shift in the wavelength maxima (448 to 430 nm) of RAS·mGDP only when $AlF_x$ is present (*35*). A smaller blue shift and intensity change are observed upon GAP binding to RAS·mGMPPNP. GAP binding also causes a $10^4-10^5$-fold increase in the rate of GTP hydrolysis (*36*), and the affinity of GAP for RAS·mGDP increases 100-fold in the presence of $AlF_x$ (*37*). The spectral changes, increased turnover, and affinity changes associated with GAP binding parallel those for the binding of AMP·$PP_i$ to ATP sulfurylase.

The $AlF_x$ effects observed in in RAS−GAP system have been traced by site-directed mutagenesis to the so-called arginine finger (*35*). Crystal structures suggest that this arginine, which is supplied by the GAP in RAS−GAP complexes, does not directly contact the tripolyphosphate chain of GTP in the ground-state complex (GAP·RAS·GTP) (*38*). The arginine swings into its catalytic position as the system moves from the ground- to the transition-state complex, at which point it interacts extensively with the atoms that undergo bonding changes in the ground- to transition-state motion. Changing this arginine to a methionine abolishes the spectral changes associated with the binding of GAP to the RAS·mGDP complex in the presence of $AlF_x$ (*35*). Thus, the change in the environment of the mant fluorophore that occurs upon moving to the transition-state complex is linked to the movement of the arginine finger into its catalytic position.

The similar effects of GAP and AMP·$PP_i$ binding, and the fact that the ATP sulfurylase isomerization establishes a new contact(s) at the $\gamma$-phosphate of GTP, suggest that ATP sulfurylase also contains an arginine finger, which is brought into contact with the $\gamma$-phosphate by the isomerization. Engaging this contact is expected to be a crucial aspect of the allostery that communicates between the sites and controls the rate of GTP hydrolysis. We have identified a candidate arginine finger reside, and will test this hypothesis using site-directed mutagenesis.

## CONCLUSIONS

Characterizing the interactions among the enzyme and ligands in ground- and transition-state complexes of ATP sulfurylase has provided insights into the nature of the rate-limiting isomerization step of the mechanism and has defined points of contact between the enzyme and reactants that are essential to the allosteric interactions that control the reactivity of the bound GTP. The affinity of the nonisomerized form of ATP sulfurylase for GTP and GDP is similar, regardless of whether activators are bound at the APS site. Activator specific interactions between the enzyme and guanine nucleotide begin to develop during the rate-limiting isomerization of the enzyme. These interactions, which change the affinity and reactivity of the nucleotide, require a change in the contact between the enzyme and $\gamma$-phosphate of GTP. The $\gamma$-phosphate contact appears to be maintained as the enzyme moves from the isomerized ground state into the transition state for $\beta,\gamma$-bond cleavage. The isomerization, which engages this contact, is elicited only by activators that mimic the E*AMP intermediate that occurs in the APS-forming reaction. This suggests that the APS reaction must reach a point at, or near, the intermediate before the allosteric contacts that drive the isomerization are formed. Thus, the isomerization results in a stepwise progression of the reactions that causes them to occur in a 1:1 stoichiometry and links their free energies.

## REFERENCES


1. Leyh, T. S. (1999) *Methods Enzymol.* (in press).
2. Roca, J., and Wang, J. C. (1994) *Cell 77*, 609−616.
3. Roca, J., and Wang, J. C. (1992) *Cell 71*, 833−840.
4. Moyer, M. L., Gilbert, S. P., and Johnson, K. A. (1998) *Biochemistry 37*, 800−813.
5. Jencks, W. P. (1989) *Methods Enzymol. 171*, 145−164.
6. Keillor, J. W., and Jencks, W. P. (1996) *Biochemistry 35*, 2750−2753.
7. Brune, M., Hunter, J. L., Corrie, J. E. T., and Webb, M. R. (1994) *Biochemistry 33*, 8262−8271.
8. Gulick, A. M., and Rayment, I. (1997) *BioEssays 19*, 561−569.
9. Liu, C., Suo, Y., and Leyh, T. S. (1994) *Biochemistry 33*, 7309−7314.
10. Liu, C., Martin, E., and Leyh, T. S. (1994) *Biochemistry 33*, 2042−2047.
11. Leyh, T. S., Vogt, T. F., and Suo, Y. (1992) *J. Biol. Chem. 267*, 10405−10410.
12. Robbins, P. W., and Lipmann, F. (1958) *J. Biol. Chem. 233*, 686−690.
13. Leyh, T. S. (1993) *CRC Crit. Rev. Biochem. 28*, 515−542.
14. Zhang, H., Varlamova, O., Vargas, F., Falany, C. N., and Leyh, T. S. (1998) *J. Biol. Chem. 273*, 10888−10892.
15. Falany, C. N., and Falany, J. L. (1996) *Cancer Res. 56*, 1551−1555.
16. Hemmerich, S., Bertozzi, C. R., Leffler, H., and Rosen, S. D. (1994) *Biochemistry 33*, 4820−4829.

17. Leyete, A., van Schijndel, H. B., Niehrs, C., Huttner, W. B., Verbeet, M. P., Mertens, K., and van Mourik, J. A. (1991) *J. Biol. Chem. 266*, 740−746.
18. Wei, J., and Leyh, T. S. (1998) *Biochemistry 37*, 17163−17169.
19. Yang, M., and Leyh, T. S. (1997) *Biochemistry 36*, 3270−3277.
20. Liu, C., Wang, R., Varlamova, O., and Leyh, T. S. (1998) *Biochemistry 37*, 3886−3892.
21. Leyh, T. S., Taylor, J. T., and Markham, G. H. (1987) *J. Biol. Chem. 263*, 2409−2416.
22. Wang, R., Liu, C., and Leyh, T. S. (1995) *Biochemistry 34*, 490−495.
23. Bourne, H. R., Sanders, D. A., and McCormick, F. (1990) *Nature 348*, 125−132.
24. Bourne, H. R., Sanders, D. A., and McCormick, F. (1991) *Nature 349*, 117−126.
25. Cleland, W. W. (1975) *Biochemistry 14*, 3220−3224.
26. Sondek, J., Lambright, D. G., Noel, J. P., Hamm, H. E., and Sigler, P. B. (1994) *Nature 372*, 276−279.
27. Coleman, D. E., Berghuis, A. M., Lee, E., Linder, A. E., Gilman, A. G., and Sprang, S. R. (1994) *Science 265*, 1405−1412.
28. Fisher, A. J., Smith, C. A., Thoden, J. B., Smith, R., Sutoh, K., Holden, H. M., and Rayment, I. (1995) *Biochemistry 34*, 8960−8972.
29. Rittinger, K., Walker, P. A., Eccleston, J. F., Smerdon, S. J., and Gamblin, S. J. (1997) *Nature 389*, 758−762.
30. Scheffzek, K., Ahmadian, M. R., Kabsch, W., Wiesmuler, L., Lautwein, A., Schmidt, F., and Wittinghofer, A. (1997) *Science 277*, 333−338.
31. Schindelin, H., Kisker, C., Schlessman, J. L., Howard, J. B., and Rees, D. C. (1997) *Nature 378*, 370−376.
32. Martin, R. B. (1996) *Coord. Chem. Rev. 149*, 23−32.
33. Wang, X., Simpson, J., and Nelson, D. J. (1995) *J. Inorg. Biochem. 58*, 29−47.
34. Mittal, R., Ahmadian, M. R., Goody, R. S., and Wittinghofer, A. (1996) *Science 273*, 115−117.
35. Lancaster, C. A., Taylor-Harris, P. M., Self, A. J., Brill, S., van Erp, H. E., and Hall, A. (1994) *J. Biol. Chem. 269*, 1137−1142.
36. Rittinger, K., Walker, P. A., Eccleston, J. F., Nurmahomed, K., Owen, D., Laue, E., Gamblin, S., and Smerdon, S. (1997) *Nature 388*, 693−697.
37. Scheffzek, K., Ahmadian, M. R., Kabsch, W., Weismuller, L., Lautwein, A., Schmitz, F., and Wittinghofer, A. (1997) *Science 277*, 333−338.

BI990216H